

FREE-FALL GRAVITATIONAL ACCELERATION MEASUREMENT USING A PNEUMATICALLY CONTROLLED CATCH-AND-RELEASE-SYSTEM IN A SEMI-ROTATING VACUUM CHAMBER

Tlou Mokobodi¹, Pieter Greeff², Oelof Kruger², Nicolaas J. Theron¹

1) University of Pretoria, Private bag X20, Hatfield, Pretoria, South Africa, 0028
(mokoboditlou@tuks.co.za, nico.theron@up.ac.za, +27 12 420 3309)

2) National Metrology Institute of South Africa, CSIR, Meiring Naude Rd, Brummeria, Pretoria, 0040
(pgreeff@nmisa.org, oakruger@nmisa.org)

Abstract

Knowledge of gravitational acceleration in metrology is required for traceable force and pressure calibrations, furthermore the redefinition of the SI base unit of kilogram requires absolute accomplishment of the gravitational acceleration. A direct free-fall gravimeter is developed using pneumatic grippers for test mass handling and a semi-rotary actuator for repositioning, *i.e.* automated re-launching. The catch and release system is powered by compressed air. This eliminates electric interferences around the test mass. A simplified method of signal capturing and processing is used on the designed gravimeter. A digital frequency trigger is implemented in the post processing algorithms to ensure that the signals are analysed from the identical effective height. The experimental results measured the site gravitational acceleration of 9.786043 ms^{-2} with a statistical uncertainty of $\pm 29 \mu\text{s}^{-2}$.

Keywords: direct free fall, gravitational acceleration, interferometer.

© 2018 Polish Academy of Sciences. All rights reserved

1. Introduction

A gravimeter is used to measure absolute gravitational acceleration g or relative gravitational force F_g . Absolute gravimeters use the *International System* (SI) base units of length and time standards to obtain the derived SI unit of acceleration (ms^{-2}), whereas relative gravimeters use the derived unit of force (N) to obtain acceleration [1]. Many fields of scientific research require knowledge of g or F_g to fulfil their mandates. In metrology the absolute measurement of g is used and favoured due to its direct shortest traceability chain to the SI base units in order to maintain high fundamental accuracy and precision [2]. Gravimeters also form an integral part of the redefinition of mass in metrology where the Watt-balance is used to achieve the mass standard [3, 4].

Historically, pendulums were the first absolute gravimeters invented and had a limited accuracy of 10^{-3} ms^{-2} , while modern free-fall gravimeters are capable of achieving accuracy in the order of 10^{-9} ms^{-2} [5]. This achievement is possible due to the availability of modern methods of measuring length and time. Free-fall gravimeters traditionally were using optical interference

system setups. In recent years there has been development in atomic free-fall gravimeters that make use of atomic interferometers [6].

In this work the *National Metrology Institute of South Africa* (NMISA) studied optical interferometer gravimeters in order to explore the possibility of developing a free-fall gravimeter. Several techniques have been developed over time on free-fall gravimeters, such as:

- Transceivers used to detect the position and time of the test mass [7].
- Optical sensors arranged at predefined lengths along the path of the test mass [8].
- An optical interferometer system used to track the falling test mass [9].

The use of an optical interferometer was preferred to other methods in this work, because the entire time and displacement of the falling test mass is captured and analysed to compute gravitational acceleration. Furthermore, different signal processing methods of analysis can be applied to a single drop to compare the results obtained with each method [10], but this was not considered.

There is a number of institutions providing commercially-ready gravimeter systems. While NMISA currently has a need for an absolute gravimeter, we have decided not to acquire a commercially-ready gravimeter; instead, we have decided to design and develop a new gravimeter from the fundamental principles using an optical interferometer system. The basic cost of doing this was already saved, since NMISA had already owned major core electronics and the optical system. Additionally, NMISA considered this development process as an important step in developing in-house knowledge of gravimeters, to also support intended future calibration services in need to render. The first prototype system developed by NMISA has been named NMISA DFFG-01.

The NMISA DFFG-01 system was developed with the future aim to provide traceable local g measurements in support of NMISA's force and pressure laboratories, which, in turn, render calibration services to the local industry and research. NMISA is also investigating the possibilities of developing a watt-balance system. This system requires high precision and accurate knowledge of gravitational acceleration; therefore it is important to understand its supporting sub-systems. The NMISA DFFG-01 currently does not meet the measurement accuracies required to carry out calibrations or to provide support in these laboratories. However, this will be resolved in the future work.

Our gravimeter uses a direct free-fall method with a vacuum chamber fully powered by pneumatic actuators that can achieve high precision positioning of the test mass through simplified handling and launching. The use of pneumatic actuators was adopted to support the need to reduce the uncertainty introduced by electric force fields reported by Rothleitner [11].

Our system uses the principle of a rotating vacuum chamber similar to the gravimeter reported by Hanada, *et al.* [12], but differs in the way that the projectile is released at the beginning of and captured after the fall. The current setup makes use of ordinary pneumatic grippers, which do result in some shock loading at the moment of actuation. However, this shock loading does not cause adverse vibration during the fall. The use of pneumatics to locate and launch the test mass ensures that it is launched and aligned precisely with the interferometer laser beam.

This paper first presents a short background on interferometric free-fall gravimetry. Then, each of the subsystems and the required integration of subsystems are discussed. Furthermore, the signal acquisition and processing method used are discussed. Lastly, the testing procedure and results of the first constructed gravimeter are presented. The results from this setup are to be improved with further recommended developmental updates of the current system.

2. Developed free-fall gravimeters

In free-fall gravimeters, a test mass is launched into space and allowed to undergo free fall, where free fall describes the displacement of an object only under the influence of the gravitational force field. The position and time of the free falling test mass are monitored and analysed to compute g [13]. There are two general system configurations: the direct free fall, and rise and fall one. Both configurations have comparable measuring capabilities with slight advantages and disadvantages that differentiate the two [9, 14]. The direct free-fall gravimeter approach was adopted, because the method of handling the test mass is relatively easy and full system automation is easily achievable.

Free-fall gravimeters consist of four major subsystems: a vacuum chamber, a laser interferometer, seismic isolation and control electronics. In the direct free-fall setup, the test mass is released in the vacuum chamber from the rest position and it is captured after a certain distance of free fall [15, 16]. The launching (or vacuum) chamber is essential to reduce the drag force on the test mass. A red He–Ne laser Michelson type interferometer, with a wavelength of λ of 633 nm is used for accurate measurement of the test mass displacement. The isolation system isolates the reference mass of the interferometer from all possible induced vibrations that can contribute to interference with the measurements [17]. The control electronics synchronizes the test mass handling, automation and data acquisition system.

The Newton's second law of motion (1) is used to calculate g , by assuming that the test mass is in ideal free fall:

$$m\ddot{z} = mg, \quad (1)$$

where \ddot{z} represents the free falling test mass acceleration in the z direction (downward) and it is defined by $\ddot{z} = d^2z/d^2t$. Integration of (1) derives (2) that is used to find the displacement of the test mass:

$$z(t) = z_0 + \dot{z}_0t + \frac{g_0}{2}t^2 + \gamma \left(\frac{1}{2}z_0t^2 + \frac{1}{6}\dot{z}_0t^2 + \frac{1}{24}g_0t^2 \right). \quad (2)$$

The gravitational gradient term γ is $3\mu\text{ms}^{-2}/\text{m}$ in practice is negligible when the measurements are performed over a short falling distance [18]. (2) then reduces to:

$$z(t) = z_0 + \dot{z}_0t + \frac{g}{2}t^2, \quad (3)$$

where: t is time; g is the local gravitational; and $z(t)$, z_0 and \dot{z}_0 are the position, the initial position and the initial velocity of the test mass at time zero. At least three time-space coordinates are required in order to solve g in direct free-fall gravimeters [18]. During the test mass drop, the interferometer outputs a fringe intensity distribution similar to the voltage signal shown in Fig. 1. The intensity signal is processed to extract the three time–displacement points required to compute the g value from the drop.

The reference mirror is placed in the isolation system. The two interfering beams result in a signal that has variable intensity due to phase difference, as a result of the relative displacement between the reference mirror and the test mass retro-reflecting mirror. This relationship is given in (4), where $\Delta\phi$ is the phase difference of the two beams and Δd is the displacement of the falling test mass [19].

$$\Delta d = \frac{\lambda}{4\pi}\Delta\phi. \quad (4)$$

Interference fringes are converted by a photo-detector into the voltage-time signal. Here, the time accuracy is vital. The average transition level from the dark to bright band or vice-versa is

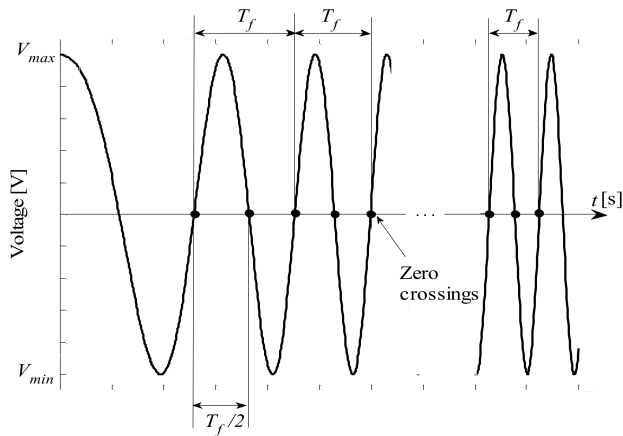


Fig. 1. A light intensity graph from the detector and converted into the electric voltage signal.

assigned the average voltage value, *i.e.* the zero crossing voltage [20]. The zero crossing points are used to calculate g . The signal produced through interference by a free falling object has a continuously increasing frequency, resulting in a chirp signal, resembling the increasing falling velocity. The chirp signal has a final frequency f_f . The decreasing wave period, T_f , corresponds to a constant phase change of $\Delta\phi = 2\pi$, and from (4) it is clear that for each full period T_f the test mass drops by $\lambda_f = 0.5\lambda$. The zero crossing method therefore enables a displacement resolution of 0.25λ .

A digitizer is used to stamp the voltage signal with real time stamp t_n points during the test mass fall. During the fall, more than 24 million time stamps t_n are generated in our setup. Zero crossing time points T_n are obtained by interpolating between two consecutive t_n points voltage values with opposite signs. The zero crossing time points T_n are stored in a new time stamp vector T , where this vector is used to construct the displacement vector using (4). Displacement-time coordinates have the form as shown below in Table 1. The detection error of the exact time of a time point directly influences the measurement accuracy [20]. The entire fringe signal is however analysed for zero crossing points; this reduces the average error accumulated due to linear interpolation.

Table 1. Time-displacement coordinates of a free-fall trajectory.

Time T_n	T_0	T_1	T_2	$T...$
Displacement	0	$\lambda/4$	$\lambda/2$...

3. NMISA DFFG-01 gravimeter

The NMISA DFFG-01 is an automated, direct free-fall gravimeter, with a release, catch, rotate by 180 degrees and release measurement cycle. The test mass handling is achieved by using pneumatic grippers and a rotary actuator. The handling cycle led to the use of a symmetrical double-sided test mass.

Figure 2 shows the system components. The gravimeter is 1.1 m above the laboratory floor, with the vacuum chamber supported and mounted to the complete supporting mechanical structure at 0.7 m in height using bearings aligned concentrically with the rotary actuator output shaft and the vacuum pump inlet. The entire vacuum chamber is semi-rotated around this axis during operation. The vacuum chamber has the total length of 0.48 m, and the length from gripper to gripper of 0.32 m with the height of free falling test mass of 0.30 m.

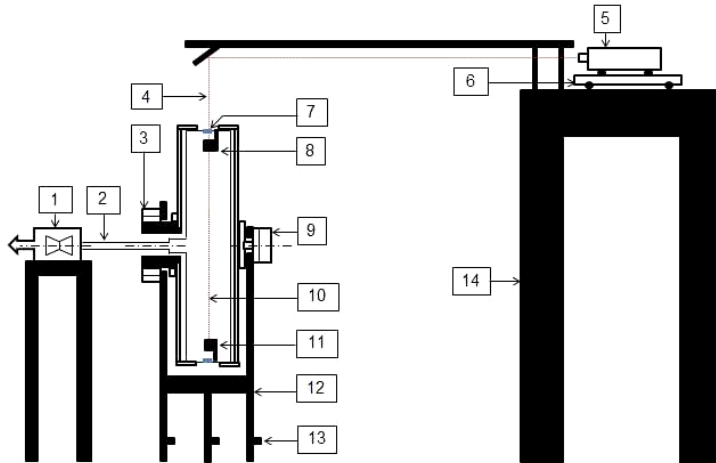


Fig. 2. The NMISA-DFFG-01 gravimeter setup, 1) vacuum pump; 2) suction duct; 3) isolating bearing; 4) laser beam path; 5) interferometer; 6) isolation table; 7) beam window; 8) gripper 1; 9) rotary actuator; 10) test mass path; 11) gripper 2; 12) stand structure; 13) adjustment knobs and 14) optical table.

Perspex and aluminium were used to construct the vacuum chamber, with O-ring seals and vacuum grease to provide sealing. The vacuum chamber is connected to a turbo-molecular vacuum pump, PFEIFFER D-35614. The vacuum pump has two pressure sensors, one is connected to the pump for pump control and the other is used for manual vacuum pressure level regulation. The prototype vacuum chamber has a limitation due to leaks and as a result the gravimeter was only evacuated to 5×10^{-2} Pa. The gravitational acceleration measurements were taken at different vacuum pressure levels to evaluate the drag force effect. Pressure ranging from 0.05 to 2.5 Pa was evaluated. The target vacuum pressure is however 10^{-4} Pa, since the drag force then becomes negligible [18].

The interferometer sensor head – Polytec OFV 505 – is mounted directly onto the air isolation table, which is placed on the optical table that shares the ground with the vacuum chamber. A DT-4048-A isolation table manufactured by Hertz is used. The intensity signal from the sensor head is processed using a Polytec vibrometer controller OFV 5000 before it is stored by the computer for signal post processing.

The gripper that launches the test mass is designed to ensure that the test mass motion depends only on the gravitational force. The gripper releases the test mass with approximately zero resultant force in the gravity plumb line direction, since the jaws release the test mass symmetrically in the direction perpendicular to the falling direction of the test mass (see Fig. 3a). The shape of the test mass is designed to enable its proper handling and control on both sides of the test mass, refer to Fig. 3b and 3c [21]. The vacuum chamber is rotated by 180 degrees, af-

ter the test mass is released by Gripper 1 and re-captured by Gripper 2, during an experimental measurement drop.

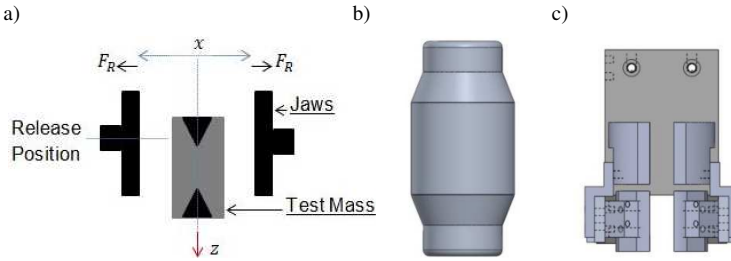


Fig. 3. The test mass launching mechanism: a) conceptualised release method; b) test mass model; c) gripper.

The automation of multiple measurements is achieved by performing the release, measure, catch and rotate sequence. A system communication diagram is shown in Fig. 4. The pneumatic actuators are controlled by the PLC (7), which is programmed by using FST (6). The electro-pneumatics station (8), which consists of solenoids valves, is used to systematically enable the logic control communication of the mechanical movement of the vacuum chamber and grippers. Storage and signal processing are done using a National Instruments card, PXI-5122, with a sampling time locked to the internal accurate clock (VCXO) with a ± 25 ppm time base accuracy. LabVIEW software is used for the data acquisition interface. The system makes use of an external electronic trigger (10) to control the start of the data acquisition. The PLC sends a voltage signal to the solenoid valve to actuate the test mass gripper release; this signal is also observed by the digitizer to initiate the acquisition.

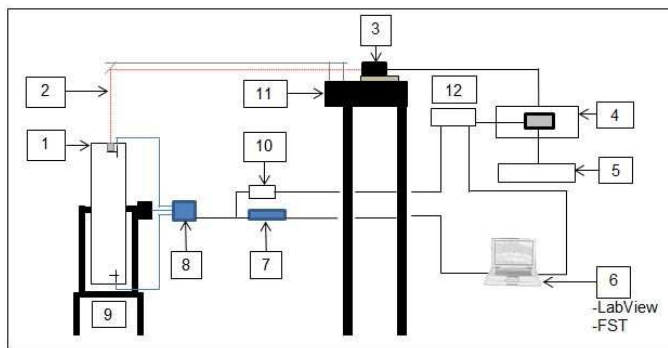


Fig. 4. A flow diagram of connecting the NMISA DFFG-01 system with all subsystems, 1) vacuum chamber; 2) laser beam path; 3) interferometer and isolation system station; 4) polytec vibrometer controller; 5) oscilloscope; 6) computer station; 7) PLC; 8) electro-pneumatic station; 9) stand structure; 10) trigger; 11) optical table and 12) digitizer.

This process was manually tuned to compensate the observed delays due to mechanical friction and compressed air travelling in the air supply lines on both actuators. Fig. 5 shows a photo of the actual setup.

Before the prototype gravimeter was built, the generation of a light intensity chirp signal by the free falling test mass as observed by the interferometer was simulated on computer, using the ideal free-fall model. This simulation was used to determine the time of falling and velocity

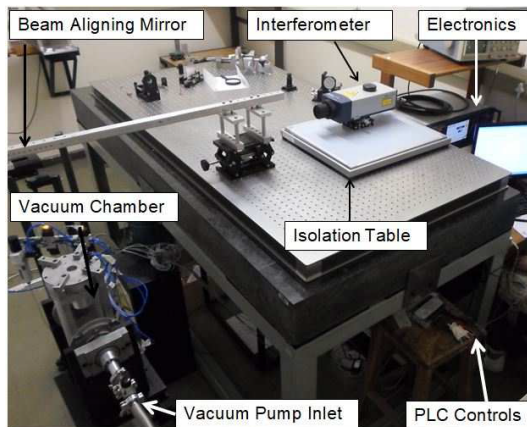


Fig. 5. Experimental system setup.

parameters, to aid in selection of a data acquisition card, for the specifications of the electronics parameters required to enable capturing and digitizing the produced interference signal and to develop signal processing algorithms for the designed gravimeter.

In processing the measured data, the signal is cropped to start at a specific frequency, to ensure that the measurements are processed from the identical height of test mass for each drop. Each instantaneous signal frequency of the drop signal corresponds to a unique test mass velocity and position each time the test mass is released from the identical position [22]. The zero crossing frequency trigger of 2.5 MHz – that corresponds to 0.00049945 m height covered by the test mass from the release position – was set to be the processing trigger point. The detection of zero crossings is then applied to extract the displacement information from the intensity signal [10, 20].

The zero crossing frequency f_{zc} observed at the highest velocity of the test mass was used as the governing frequency for selection of electronics. This is required to enable the signal mapping of the entire falling height. The f_{zc} is calculated in (5):

$$f_{zc} = \frac{V_1}{0.25\lambda} = \frac{2.203 \text{ ms}^{-1}}{0.25 \times 633 \times 10^{-9} \text{ m}} = 13.92 \text{ MHz} \approx 14 \text{ MHz}. \quad (5)$$

The highest intensity signal frequency is therefore $f_s = 7 \text{ MHz}$.

The detected signal is sampled at a constant sampling rate. However, the intensity signal has a continuously increasing frequency over the projectile falling period, therefore time coordinates of zero crossing rarely occur at a sample point. As a result interpolation is required to extract the zero crossings. In the application of the free-fall gravimetry, the intensity signal therefore must be sampled with the frequency at least 7 times greater than the zero crossing one [11]. A 100 MHz and a 14-bit resolution card are therefore used for data acquisition.

4. Evaluation

The system was evaluated against the CG-5 Autograv, the Council of Geo-sciences of South Africa commissioned gravimeter. The CG-5 was brought to the NMISA and the measurement results of the two systems were compared after performing concurrent measurements. However,

the CG-5 is a relative gravimeter, and is referenced to the Council of Geo-sciences base station in Pretoria, situated 1.6 km away from the NMISA laboratories. At the base station the absolute gravity is known and measurements are referenced to this value. The CG-5 measured the local NMISA g value $9.7860981 \text{ ms}^{-2}$ with $\pm 0.5 \mu\text{ms}^{-2}$ standard deviation; this value is taken as the reference value for validating the NMISA DFFG-01.

Multiple drops of 10 were launched continuously to form a set of measurements within a period of 3 minutes. The sets were taken continuously over 8 hours with the system settling time of 30 minutes in between. The mean g value was calculated for each set as g_s . Six sets were used in the results reported in this work. The gravitational acceleration g_p was calculated using the mean gravitational acceleration of all the drops in the six sets. The population standard deviation σ_p was calculated using sample values g_s . The set sample standard deviation σ_s was calculated using the drops in each set. The experimental results are shown in Table 2.

Table 2. The results of experimental gravitational acceleration measurements with each set comprising multiple drops at 0.05 Pa operating pressure.

Set (n)	Number of drops	Set Mean [ms^{-2}]	Set standard deviation [ms^{-2}]
1	8	9.786 16	0.001 28
2	9	9.785 94	0.000 63
3	8	9.786 06	0.001 22
4	8	9.785 97	0.000 65
5	8	9.786 08	0.000 75
6	9	9.786 02	0.000 87
	g_p	9.786 04	
	σ_p	0.000 07	

The set gravitational acceleration g_s and standard deviation σ_s results of elements contained in each set and the reference value of NMISA site using CG-5 are shown in Fig. 6.

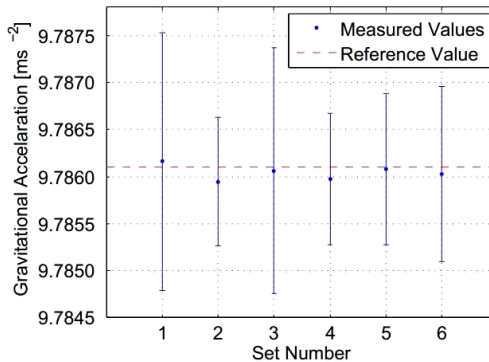


Fig. 6. Gravitational acceleration and standard deviation for sets 1 to 6 compared with the reference value acceleration measured by CG-5.

The standard deviation of the measured acceleration by the gravimeter in each set covered the reference g value. Furthermore, the average g value measured with the NMISA DFFG-01, in each of the six sets, was within a tolerance error band of 1.55×10^{-5} on either side of the reference

value. The contribution of systematic uncertainties by the current system was not evaluated, however the overall type A statistical standard uncertainty u of the equipment was calculated from the measured results presented in Table 2, using (6).

$$u = \frac{\sigma_p}{\sqrt{n}} = \frac{0.000071}{\sqrt{6}} = 29 \mu\text{s}^{-2}. \quad (6)$$

The release, catch and rotate method necessitated the use of a double-sided test mass. However, the *centre of mass* (COM) of the test mass does not coincide with the *optical centre* (OC) of both retroreflector prisms mounted in the test mass, see Fig. 7.

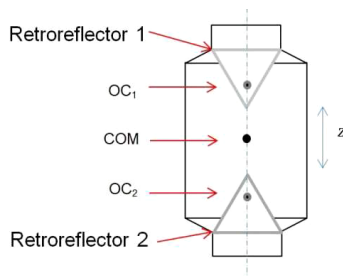


Fig. 7. A schematic design view of the test mass.

A systematic error is associated with the test mass rotation during free fall [23]. The test mass is likely to rotate around its COM. When COM and OC coincide, the quality of the measurements improves as the interferometer will be measuring the motion of the COM of the test mass. Despite the offset displacement of the OC in the falling z direction, the COM coincides with the OC in the horizontal plane, therefore the test mass must be launched in such a way as to ensure that nearly perfect launching is achieved.

A possible solution to this problem is to have a ring with a suitable tolerance fitted around the test mass that can be shifted in the axial direction relative to the test mass, in order to change the COM position to coincide with the OC of the upper (active) retroreflector. The current test mass, when used on the rotated vacuum chamber, still increases the achievable rate of measurements.

5. Conclusion

The presented gravimeter measured g successfully with a standard statistical uncertainty of $\pm 29 \mu\text{m}^{-2}$. In free-fall gravimeter applications, geometrical control of the test mass is significant as the interferometry measurements depend solely on the orientation of the test mass optics. The use of air-powered parallel grippers to perform the alignment, launching and capturing of the test mass in the design reduces the experimental error contributed by the electromagnetic forces associated with the alternative use of electric controllers employed in mechanical structures. The successful measurements and current accuracy of g obtained using this gravimeter showed that the method employed in the design has a potential for improvements in the future development in which fast and simple experiments can be achieved. The implemented zero crossing algorithms resulted in acceptable readings, and they will be used in the future development.

The vacuum chamber pressure showed a direct effect on g measurements during the evaluation of the gravimeter. The future work should be focused on improving the method of reducing

and maintaining acceptable required vacuum chamber pressure of 10^{-4} Pa or less to improve the measurement results through reduction of measurement variation and to obtain a good approximation.

Acknowledgements

The authors would like to acknowledge NMISA, which provided the sponsorship for this project, and the department of Mechanical and Aeronautical engineering of the University of Pretoria.

References

- [1] Nabighian, M.N., Ander, M.E., Grauch, V.J., Hansen, R.O., LeFehr, T.R., Li, Y., Pearson, W.C., Pierce, J.W., Phillips, J.D., Ruder, M.E. (2005). Historical development of the gravity method in exploration. *Geophysics*, 70(6), 63ND–89ND.
- [2] Darling, D. (2006). *Gravity's Arc: The story of gravity from Aristotle to Einstein and beyond*. New Jersey: John Wiley and Sons.
- [3] Stock, M. (2011). The watt balance: determination of the Planck constant and redefinition of the kilogram. *Philosophical transactions of the royal society*, 369(2011), 3936–3953.
- [4] Sanchez, C.A., Wood, M.B., Green, R.G., Liard, J.O., Inglis, D. (2014). A determination of Planck's constant using NRC watt balance. *Metrologia*, 51(2014), S5–S14.
- [5] Krynski, J. (2012). Gravimetry for geodesy and geodynamics – brief historical review. *Reports on Geodesy*, 92(1), 1–16.
- [6] Gillot, P., Cheng, B., Merlet, S., Pereira Dos Santos, F. (2009). The LNE-SYRTE cold atom gravimeter. *PSL Research University*. Paris: PSL Research University, 1–3.
- [7] AbdElazem, S., Al-Basheer. W. (2015). Measuring the acceleration due to gravity using IR transceiver. *European Journal of Physics*, 36, 45017.
- [8] Abellan-Garcia, F.J., Garcia-Gamuz, J.A., Valerdi-Perez, R.P., Ibanez-Mengual, J.A. (2012). Gravity acceleration measurement using a soundcard. *European Journal of Physics*, 33, 1271–1276.
- [9] Faller, J.E., Marson, I. (1988). Ballistic Methods of Measuring g – the Direct Free-Fall and Symmetrical Rise and Fall Methods Compared. *Metrologia*, 25, 49–55.
- [10] Svitlov, S., Maslyk, P., Rothleitner, C., Hu, H., Wang, L.J. (2010). Comparison of three digital fringe signal processing methods in ballistic free-fall absolute gravimeter. *Metrologia*, 47(6), 677–689.
- [11] Rothleitner, C. (2008). *Ultra-High Precision, Absolute Earth Gravity Measurements*. Dissertation. Max Plank Research Group.
- [12] Hanada, H., Tsubokawa, T., Takano, S., Tsuruta, S. (1987). New design of absolute gravimeter for continuous observations. *Review of Scientific Instruments*, 58(4), 669–673.
- [13] D'Agostin, G., Desogus, S., Germak, A., Origlia, C., Quagliotti, D., Berrino, G., Corrado, G., d'Errico, V., Ricciardi, G. (2008). The new IMGC-02 transportable absolute gravimeter: measurement apparatus and applications in geophysics and volcanology. *Annals of Geophysics*, 51(1), 39–49.
- [14] Cook, A.H. (1965). The absolute determination of acceleration due to gravity. *Metrologia*, 1(3), 84–113.
- [15] Bell, G.A., Gibbings, D.L.H., Patterson, J.B. (1973). An absolute determination of the gravitational acceleration at Sydney, Australia. *Metrologia*, 9, 47–61.

- [16] Niebauer, T.M., Hollander, W.J., Faller, J.E. (1992). Absolute Gravity Inline Measuring Apparatus Incorporating Improved Operating Features. *Micro-g Solution*, 45(US005351122A), 1–18.
- [17] Hammond, J.A. (1970). *A laser-interferometer system for the absolute determination of the acceleration of gravity*. PhD Thesis. Colarad: University of Colorado.
- [18] Torge, W. (1989). *Gravimetry*. New York: Walter de Gruyter.
- [19] Hariharan, P. (2007). *Basics of Interferometry*. 2nd ed. Sydney: Elsevier.
- [20] Svitlov, S., Rothleitner, C., Wang, L. (2012). Accuracy assessment of the two-sample zero-crossing detection in a sinusoidal signal. *Metrologia*, 49, 413–424.
- [21] Ilango, S., Soundararajan, V. (2007). *Introduction to Hydraulics and Pneumatics*. India: Prentice-Hall of India Private Limited.
- [22] Ludger, T. (2003). Precise definition of the effective measurements height of the free-fall absolute gravimeter. *Metrologia*, 40, 62–65.
- [23] Rothleitner, C., Francis, O. (2010). On the influence of the rotation of a corner cube reflector in absolute gravimetry. *Metrologia*, 47, 567–574.